BUCHAREST UNIVERSITY

EXPERIMENTAL PARTICLE PHYSICS GROUP

14

UBPub.EPPG-Phys-27

Fermilab Library 0 1160 0049279 7

UBPub.EPPG/Phys.27
July 1995

KAON ELECTROPRODUCTION AT CEBAF

Tatiana ANGELESCU, Alexandru MIHUL, Liliana TEODORESCU
Faculty of Physics,University of Bucharest, Romania

O.K. BAKER, Gabriel NICULESCU, Ioana NICULESCU
Hampton University and CEBAF,Virginia, USA

ABSTRACT

Kaon electroproduction is used for studying hadron structure via virtual photon interaction.Model independent separation of the longitudinal and transverse cross sections will be achieved in this experiment.

For optimizing the experimental conditions a program has been written. It computes kinematics conditions and the counting rates in the two arm spectrometer taking into account the spectrometer acceptance. The conclusions have been used in the proposal of the experiment accepted to be performed at CEBAF in 1996.

FERMILAB
OCT
LIBRARY

NAME WOLBERS 6807 120

KAON ELECTROPRODUCTION AT CEBAF

T. Angelescu[1], O.K. Baker[2], A. Mihul[1], G. Niculescu[2], I. Niculescu[2], L. Teodorescu[1]

[1] Faculty of Physics, Bucharest University, Romania
[2] Hampton University, Hampton, VA, USA

1 INTRODUCTION

Electroproduction is an efficient tool for studying particle structure. Quantum electrodynamics was prooved to be valid for leptons up to a very high order and electromagnetic interaction can be treated in the one photon approximation (OPA) due to the small value of the coupling constant α.

Using these well established assumptions, one can write the differential cross section for unpolarized electrons on an unpolarized target [1]. It has four components which can be separated using suitable experimental configurations:

$$\frac{d\sigma}{dt} = \sigma_U + \epsilon\sigma_L + \epsilon\cos(2\phi)\sigma_{TT} + \left[\frac{\epsilon(\epsilon+1)}{2}\right]^{1/2}\cos\phi\sigma_{LT} \qquad (1)$$

where ϕ is the angle between the scattering and production planes, t is the four-momentum transfer from the virtual photon to the kaon, ϵ is the polarization of the virtual photon.

The kaon cross section components are related to the virtual photon helicity amplitudes:

1. σ_U is the cross section for transverse unpolarized virtual photons and can be compared with unpolarized real photon cross section for very small four-momentum transfer values.

2. σ_L is the cross section for longitudinal polarized photons and is an attribute of the virtual photons only. The longitudinal virtual photons having zero helicity are able to produce pions or kaons moving along their direction. If dominated by the kaon pole contribution, σ_L can provide a value of the kaon form factor by using the Chew Low extrapolation method.

3. σ_{TT} describes the modification in the cross section if the transverse photons are partially polarized.

4. σ_{LT} is the result of the interference between longitudinal and transverse components.

For zero four-momentum transfer, i.e. for real photons, ϵ vanishes and the virtual cross section becomes the photoproduction cross section.

The separation of the four components of the cross section can provide valuable information about the photoproduction with real and virtual photons. The advantage of the virtual photon reactions is the fact that the polarization is precisely known and can be varied in large limits by choosing different kinematical configurations. The separation of the four cross sections does not involve model dependent methods. This is the most important advantage of the experiment proposed at CEBAF by our group and described in [5].

This paper presents a program performing the kinematical computations, the counting rate and trigger efficiency evaluations depending on the experimental possibilities of the project in reaching the proposed goal. The program takes into account the two arm spectrometer acceptances neglecting multiple scattering and detector resolution.

The cross sections used in counting rate evaluations were based on the previous experimental data obtained by other groups and extrapolated for our kinematical configurations. We used also theoretical predictions for the cross sections but we did not rely on these values in computing counting rates because many models involve parameters (coupling constants, form factors) obtained by the authors using the same experimental data.

The program can be used for computing background diagram contributions. For Λ and Σ channels separation the missing mass distribuiton can be modeled taking into account radiative corrections or spectator distribuitons in other light nuclei.

2 MODELING TWO ARM SPECTROMETER FOR K^+ ELECTROPRODUCTION

The study of kaon electroproduction on protons and deuterons at CEBAF HMS SOS facility benefits of some characteristics which lead to much more complete and reliable results than those obtained in the previous experiments [2],[3],[4]:

1. The first and most important new contribution of the experiment is the separation of the transverse and longitudinal cross sections by varying, in the same experiment, the polarization ϵ in a large range ($0.28 \leq \epsilon \leq 0.86$).

2. The electron four-momentum transfer Q^2 range extends from 0.5 $(\mathrm{GeV}/c)^2$ up to 2.0 $(\mathrm{GeV}/c)^2$. Using the Chew Low extrapolation technique for the longitudinal cross section one can obtain a Q^2 dependence of the kaon form factor on a large range and thus test different theoretical predictions.

3. The ratio of the cross section for $K^+\Lambda$ and $K^+\Sigma^0$ channels in the Bjorken variable range $0.2 \leq x \leq 0.5$ can give an answer about the strangeness content of the proton as predicted by Nachtmann[6].

4. The measurement of the out of plane kaon electroproduction for $-10° \leq \phi \leq 10°$ with a precision of 0.06° leads to the separation of σ_{LT} and σ_{TT} for t in the range 0.11 to 0.50 $(GeV/c)^2$.

5. The uncertainty on kinematic parameter values is about 1% and the uncertainty on the cross section is less than 5%. In this way the errors of the separated cross sections are smaller than that obtained in previous experiments.

2.1 Phase space limitations for the CEBAF two arm spectrometer

The limitations imposed by the experimental conditions define the range of variation for the variables: Q^2, W, t, ϵ. The proposal[5] gives the experimental conditions which define the kinematical limits:

1. the scattered electron angle can vary from 14.5 to 61.4 degrees
2. the produced kaon can be detected between 13.5 and 23.6 degrees
3. the electron momentum can be varied between 0.7 and 2.4 GeV with 20% acceptance
4. the kaon momentum can be varied between 1.0 and 1.7 GeV with 40% acceptance

The K^+ electroproduction starts with a threshold value for the invariant mass of the $K\Lambda$ system, W:

$$W_{min} = m_\Lambda + m_K = 1.61 GeV \tag{2}$$

This limitation will fix the minimum energy of the virtual photon ν:

$$\nu_{min} = \frac{W^2_{min} + Q^2 - M^2}{2M} \tag{3}$$

where M is the proton mass.

The Q^2 value is limited by the electron scattering angle and the beam energy. The minimum scattering angle (14.5 deg.) leads to the minimum Q^2 value.

$$Q^2_{min} = E_e(E_e - \nu)\sin^2(\theta_{min}/2) \tag{4}$$

where E_e is the beam energy.

The minimum four momentum transfer from the virtual photon to the kaon, t_{min}, depends on W, Q^2, and E_e. Its dependence on the kaon momentum p_K for different Q^2 values is given in Fig. 1. The Chew Low extrapolation of the longitudinal cross section depends on the minimum four momentum transfer t_{min}. In order to obtain smaller t_{min} values we need higher W values. Especially for high Q^2, W is limited by the angular range of the kaon arm spectrometer.

To obtain high Q^2 values we are constrained to work near the threshold ($W \approx 1.7$ GeV) for small beam energy.

The Bjorken variable x is limited to a short range of values, $0.2 \leq x \leq 0.5$, not interesting for deep inelastic scattering studies. However measurements of the $K\Lambda$ and $K\Sigma^0$ cross sections with high precision extend the possibility to check the strangeness content of the proton given by the theoretical models[6].

As one of the most important goals of this experiment is the transverse/longitudinal cross section separation, we show in Fig.2 the dependence of σ_{tr}, σ_L on t given by Williams and Cotanch [7]. Using these cross section values we computed the counting rates for a set of measurements at low t values which would permit the determination of the kaon form-factor.The kinematical configurations and the corresponding counting rates are given in Table 1 and Table 2.

2.2 Kaon electroproduction cross sections

Table I gives the kinematical settings chosen in the experiment for the transverse longitudinal cross section separation in the kaon electroproduction on nucleon:

$$e + p \rightarrow e' + K^+ + \Lambda(\Sigma^0) \tag{5}$$

$$e + n \rightarrow e' + K^+ + \Sigma^- \tag{6}$$

At these values for W all other strange particle production channels are closed (for example K^+K^-N). The pion rejection achieved using time-of-flight and Cherenkov counter in the kaon arm will be about 100 to 1. In the electron spectrometer arm (HMS) the pion rejection will be about 500[5]. Therefore, the background in the two arm coincidence experiment will be due to the reactions (5) and (6) with different kinematical configurations accepted by the spectrometer during the resolution time of the coincidence scheme.

Counting rate evaluation in the two spectrometer arm should start with the kaon cross sections of the reactions investigated. We chose as input the data obtained by Bebek[3], as being the most recent and reliable. $\frac{d\sigma}{d\Omega_K}$ has been extrapolated to the kinematical settings used in our experiment(W,Q^2,t), by using the extrapolation law [3]:

$$\frac{W\,(W^2 - M^2)\,(Q^2 + a)}{p_K^{CMS}\,e^{2\,bt}}\left(\frac{d\sigma}{d\Omega_K}\right)^{CMS} = const. \tag{7}$$

with $a = 2.67$ for Λ production
and $a = 0.79$ for Σ^0 production
For evaluating the counting rate we used the following cross sections:

2.2.1 Kaon electroproduction cross section

The laboratory system cross section for reactions (5) and (6) is given by:

$$\sigma(e, e'K) = \frac{d^3\sigma}{dE'_e d\Omega_e d\Omega_K} = \Gamma(\frac{d\sigma}{d\Omega_K})^{CMS} \frac{d(\cos\theta^{CMS})}{d(\cos\theta)} \tag{8}$$

$$\Gamma = \frac{\alpha/4\pi^2 E'(W^2 - M^2)}{EMQ^2(1-\epsilon)} \tag{9}$$

is the virtual photon flux
$(\frac{d\sigma}{d\Omega_K})^{CMS}$ is the extrapolated cross section according to[3]. In computing the cross section for reaction (6),we made the assumption:

$$\sigma(\gamma_v n \Rightarrow K^+\Sigma^-) = \sigma(\gamma_v p \Rightarrow K^+\Sigma^0) \tag{10}$$

which is supported by the experimental data of Bebek[3].

The cross section given by (8) was used to evaluate the coincidence counting rate.

2.2.2 Elastic electron scattering cross section

The elastic electron scattering on nucleons has been computed using the relation [8]:

$$\sigma(e, e') = \frac{d\sigma}{d\Omega_e} = \sigma_{Mott} \left(\frac{G_E^2 + \frac{Q^2}{4M^2} G_M^2}{1 + \frac{Q^2}{4M^2}} + \frac{Q^2}{2M^2} G_M^2 \tan^2(\theta/2) \right) \tag{11}$$

where G_E and G_M are the electric and magnetic form factors of the target(proton or neutron) and σ_{Mott} is the Mott cross section:

$$\sigma_{Mott} = \frac{\alpha^2 \cos^2\theta/2}{4E_e^2 \sin^4\theta/2} \frac{1.}{1. + 2(E_e/M)\sin^2\theta/2} \tag{12}$$

The cross section computed with relation (11) has been used in evaluating electron arm counting rate and consequently the background coincident events.

2.2.3 Kaon arm integrated cross section

We integrated the $(e, e'K)$ cross section expressed as a function of W andQ^2 for all K^+ momentum values accepted by the kaon arm spectrometer at a given angle.

$$\sigma(e, K) = \int dW^2 \int \Gamma'(\frac{d\sigma}{d\Omega_K})^{CMS} \frac{d(\cos\theta^{CMS})}{d(\cos\theta)} dQ^2 \tag{13}$$

where

$$\Gamma' = \frac{\alpha}{16\pi^2} \frac{W^2 - M^2}{E^2} \frac{1}{M^2Q^2(1-\epsilon)} \tag{14}$$

$$W_{min} = M_\Lambda + M_K \tag{15}$$

$$W_{max} = s^{1/2} - M_e \tag{16}$$

$$Q^2_{min} = 0 \tag{17}$$

$$Q^2_{max} = 4(E, E'_e)^{GCMS} \tag{18}$$

GCMS is the general center of mass(e,N) system.

This integrated cross section will give the counting rate in the kaon arm for accidental coincidences.

2.3 Counting rates

2.3.1 Coincidence counting rate

This counting rate is determined by true coincidence between the scattered electron and the K^+ in reactions(5) and(6). We evaluated it using the $\sigma(e, e'K^+)$ given by (8).

The coincidence rate is:

$$R_c = \sigma(e, e'K^+)\exp(-Lm_K/p_K\tau_K)\Delta E_e \Delta\Omega_e \Delta\Omega_K n_e n_t t \tag{19}$$

where

- $n_e = I/q_e$,I is the beam intensity
- n_t is the density of nuclei in the target
- t is the target length
- ΔE_e is the energy acceptance in the electron arm
- $\Delta\Omega_e$ is the angular acceptance in the electron arm
- $\Delta\Omega_K$ is the angular acceptance in the kaon arm

The exponential term defines the probability that the kaon does not decay before detection.

2.3.2 Electron arm counting rate

The electron arm counting rate is evaluated by using the elastic electron scattering cross section given by (11).It has been computed separately for protons and neutrons according to the relation:

$$R_e = \frac{d\sigma}{d\Omega_e} n_e n_t t \Delta\Omega_e \tag{20}$$

2.3.3 Kaon arm counting rate

The kaon arm counting rate has been evaluated according to the procedure described in (2.2.3) with $\sigma(e, K)$ given by (13):

$$R_K = \sigma(e, K) n_e n_t t \Delta\Omega_K \exp(-L M_K / p_K \tau_K) \tag{21}$$

Using these rates we computed the ratio of accidental and true events for a given resolution time (τ_{res}) in the coincidence scheme:

$$\frac{A}{T} = \frac{\tau_{res} R_e R_K}{f R_e} \tag{22}$$

f is the duty factor ($f = 1$ for CEBAF) The ratio $\frac{A}{T}$ is an important characteristic of the experiment: it defines the efficiency of the triggering system.

3 PROGRAM RESULTS AND FACILITIES

The program for the computation of kinematics,cross sections and counting rates starts with the reactions (5) and (6) and combines the cross section data to obtain rates for reactions on nuclei without taking into account the nuclear interaction.

$$e + {}^A_Z N \rightarrow e' + K^+ + X \tag{23}$$

We applied the model to deuterium where the binding energy is small. Table 4 shows the computed counting rates for the kinematical settings shown in Table 3 for deuterium electroproduction.It is seen that,except the small Q^2 values where $\frac{A}{T}$ is still high,we can reduce the accidental events to less than 10%.

Using the computed values of the coincidence counting rate and the accidental on true events ratio we can optimize the experimental conditions in respect with the kinematical variables.As an example we show in Fig.3 the dependence of the rates on Q^2 for W=1.84 GeV at the beam energy of 3.2 GeV. Fig.4 shows the rate dependence on W for the same beam energy and for Q^2=2.0$(GeV/c)^2$. We can see a steep decrease of the coincidence rate with Q^2,as expected. The ratio $\frac{A}{T}$ does not vary very much with W and is flat beyond W=1.7 GeV.According to this behaviour,the kinematical configurations in the experiment have been chosen at about the same value of W (1.84 GeV) for Q^2 as large as possible.For higher energies, the kinematics would permit better separation in ϵ.

4 CONCLUSIONS

Preliminary computations for the experimental study of kaon electroproduction have been performed in order to optimize the kinematical set-ups and evaluate the counting rates,statistical errors,background contributions and the running time for each set-up.The program has been used in run-plan evaluations for the experiment accepted to be performed at CEBAF in 1996.[5]

References

[1] J.Martino An Introduction to Electron Scattering Hadronic Physics with MultiGeV Electrons.Les Houches 6-15 febr.1990 NY,1991

[2] G.N.Brown et al Phys.Rev.Lett.28(1972)1086

[3] C.J.Bebek et al Phys.Rev.D15(1977)594

C.J.Bebek et al Phys.Rev. D15(1977) 3082

[4] P.Browel et al Phys.Lett 69B(1977)253

P.Browel et al Z.Physik C,Particles and Fields 3(1979)101

[5] O.K.Baker et al Longitudinal/Transverse Cross Section Separation in $p(e,e'K)A(\Sigma)$ for $0.5 \leq Q^2 \leq 2.0(GeV/c)^2$, $W \geq 1.7GeV$ and $t_{min} \geq 0.1(GeV/c)^2$ CEBAF Proposal E 93-018,1993

[6] O.Nachtmann Nucl.Phys. B74(1974)422

[7] R Williams private communication (1993)

[8] J.W Lightbody,J.S.O'Connell Comp.Phys.,May/June (1988)57

List of Figures

Fig. 1 t_{MIN} dependence on kaon laboratory momentum for different Q^2 values

Fig. 2 σ_T and σ_L dependence on t according to Williams and Cotanch model[7]

Fig. 3 Counting rates dependence on Q^2 for W = 1.84 GeV and E_e = 3.2 GeV.

Fig. 4 Counting rates dependence on W for Q^2 = 2$(GeV/c)^2$ and E_e = 3.2GeV

Kine.	Q^2	E_e	E'_e	θ_e	θ_γ	W	p_K	ϵ	t
t1b	0.65	3.5	1.70	19.03	16.31	1.90	1.40	0.75	0.228
t2b	0.50	3.5	1.70	16.68	14.57	1.94	1.43	0.75	0.169
t3b	0.35	3.5	1.69	13.96	12.41	1.98	1.46	0.76	0.121
t4b	0.75	3.5	1.46	22.10	14.33	1.99	1.66	0.67	0.214

Table 1: Kinematical Configurations for Cross Section t Dependence

Kine.	I (μA)	$R_c(e,e'K)$ (Hz)	$R_e(e,e')$ (kHz)	$R_K(e,K)$ (kHz)	A/T $\tau_{res} = 2ns$
t1b	30.	0.693	19.60	0.739	0.042
t2b	30.	1.126	48.99	0.821	0.070
t3b	30.	1.970	153.75	0.910	0.142
t4b	30.	0.430	8.30	0.919	0.035

Table 2: Counting Rates for Cross Section t Dependence

Kine.	Q^2	E_e	E'_e	θ_e	θ_γ	W	ν	ϵ	x
1.a	0.50	2.4o	0.80	29.56	13.04	1.84	1.60	0.54	0.17
1.b	0.50	3.20	1.57	18.25	16.31	1.84	1.60	0.76	0.17
1.c	0.50	4.00	2.39	13.16	18.10	1.84	1.60	0.86	0.17
2.a	1.00	2.40	0.61	49.20	12.76	1.81	1.80	0.36	0.30
2.b	1.00	3.20	1.38	27.69	18.08	1.81	1.80	0.66	0.30
2.c	1.00	4.00	2.19	19.48	20.77	1.81	1.80	0.80	0.30
3.a	1.50	2.40	0.61	61.37	12.98	1.69	1.85	0.28	0.43
3.b	1.50	3.20	1.34	34.39	19.91	1.69	1.85	0.61	0.43
3.c	1.50	4.00	2.23	23.42	23.56	1.69	1.85	0.78	0.43
4.a	2.00	3.20	0.79	53.14	13.03	1.84	2.40	0.34	0.44
4.b	2.00	3.50	1.09	42.51	15.33	1.84	2.40	0.46	0.44
4.c	2.00	4.00	1.59	32.67	17.90	1.84	2.40	0.60	0.44

Table 3: Kinematical settings for $d(e,e'K^+)\lambda, \Sigma^0, \Sigma^-$

Kine.	I (μA)	$R_c(e,e'K)$ ($10^{-2}Hz$)	$R_e(e,e')$ (kHz)	$R_K(e,K)$ (kHz)	A/T
1.a	10	6.50	5.30	1.33	0.11
1.b	10	19.1	24.0	1.22	0.15
1.c	10	38.0	56.5	1.19	0.17
2.a	20	2.14	0.40	3.32	0.06
2.b	20	7.20	2.78	2.70	0.10
2.c	20	15.4	7.50	2.10	0.12
3.a	30	0.56	0.09	2.34	0.04
3.b	30	1.94	0.70	1.90	0.07
3.c	30	4.10	1.97	1.70	0.08
4.a	30	0.94	0.06	8.52	0.05
4.b	30	1.44	0.12	7.45	0.06
4.c	30	2.47	0.28	6.36	0.07

Table 4: Coincidence and Single Rates for $d(e,e'K^+)\Lambda, \Sigma^0, \Sigma^-$

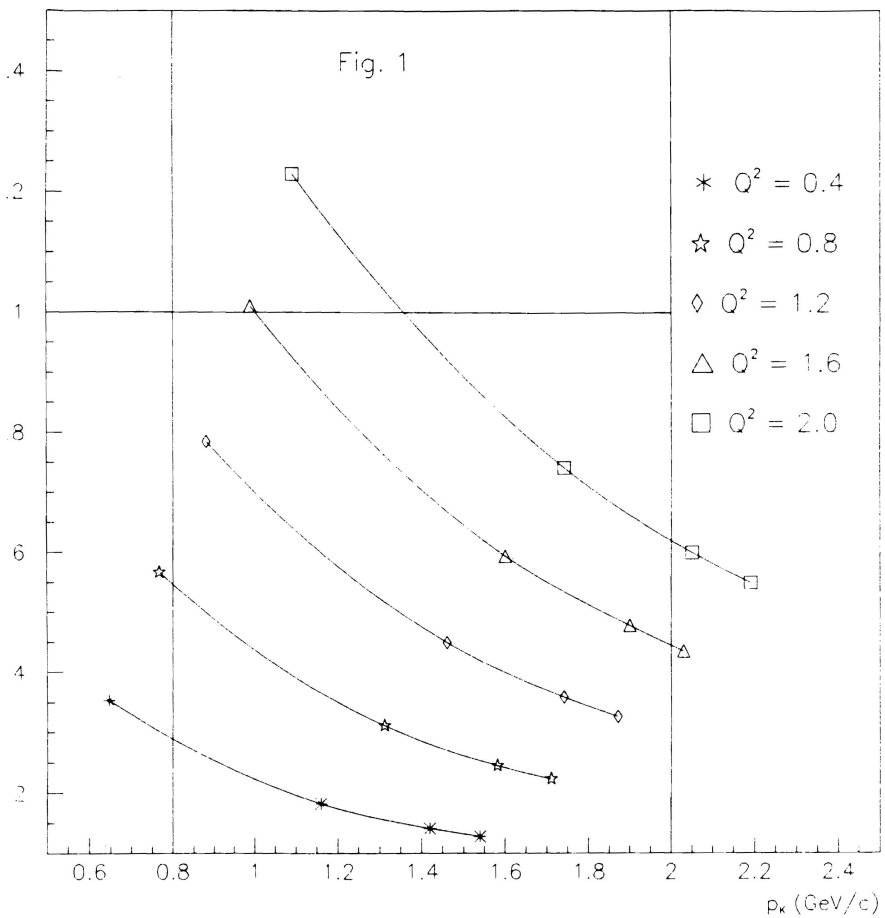
Fig. 1
Q^2 = 0.4
Q^2 = 0.8
Q^2 = 1.2
Q^2 = 1.6
Q^2 = 2.0
p_K (GeV/c)

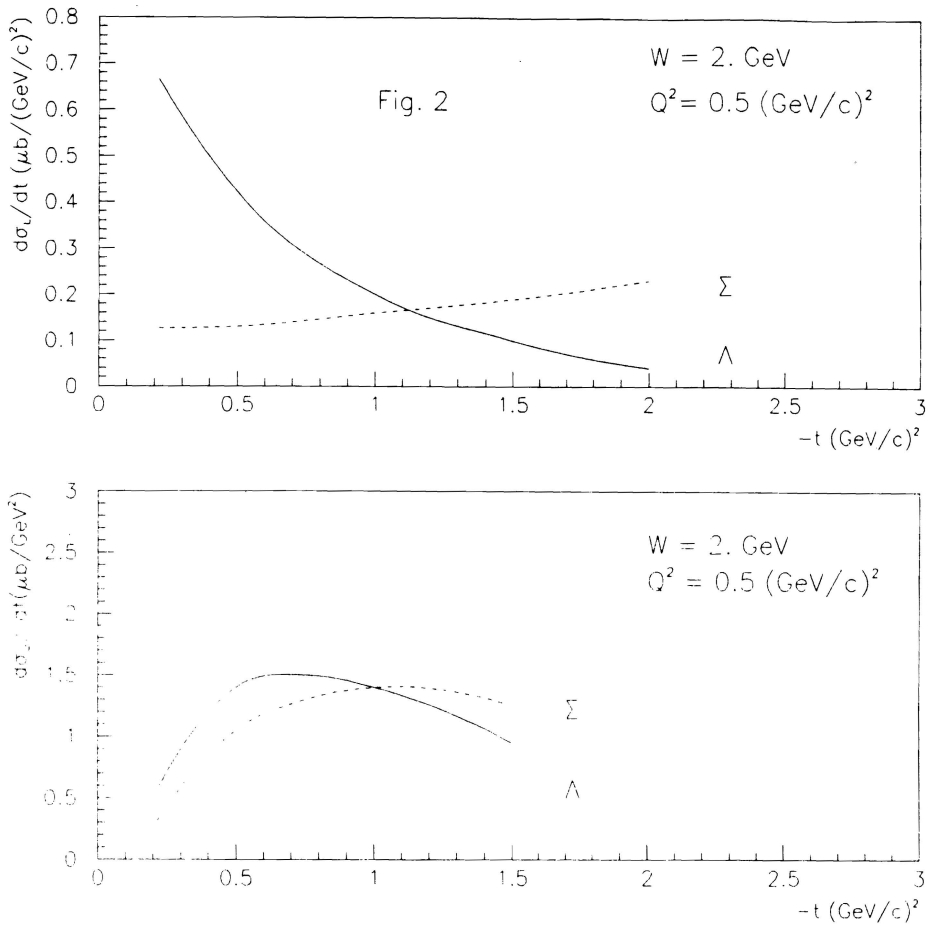
Fig. 2
W = 2. GeV
Q^2= 0.5 (GeV/c)^2
$d\sigma_L/dt$ (μb/(GeV/c)^2)
Σ
Λ
−t (GeV/c)^2
W = 2. GeV
Q^2 = 0.5 (GeV/c)^2
Σ
Λ
−t (GeV/c)^2

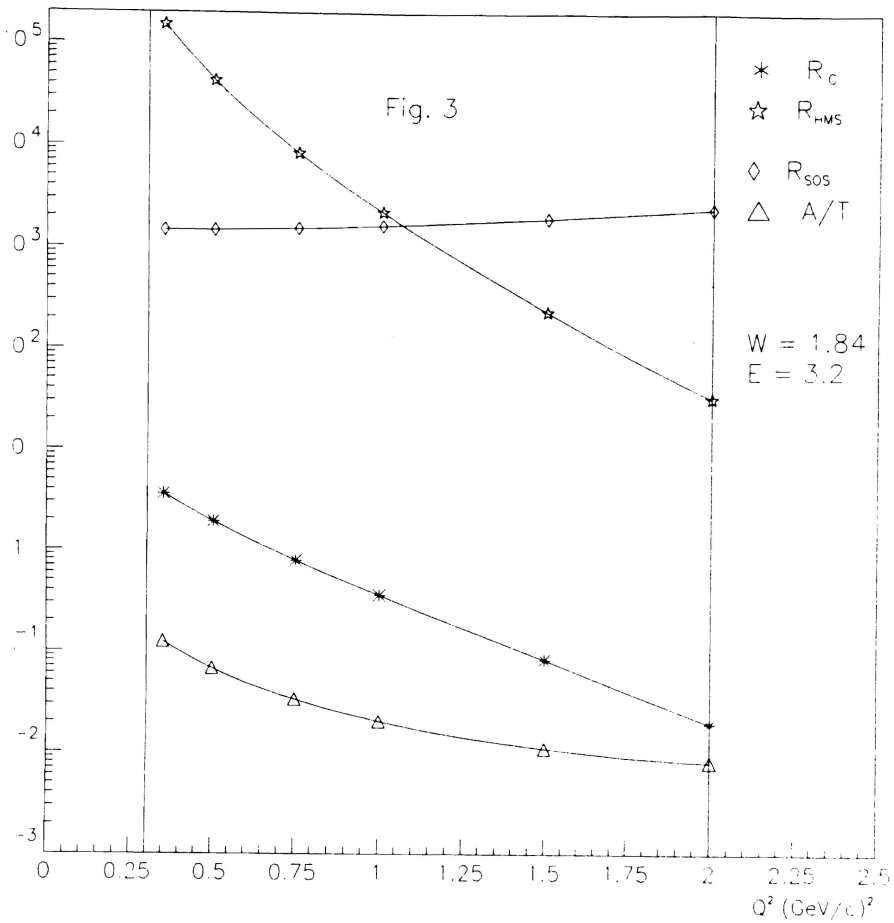
Fig. 3
R_c
R_{HMS}
R_{SOS}
A/T
W = 1.84
E = 3.2
Q^2 (GeV/c)^2

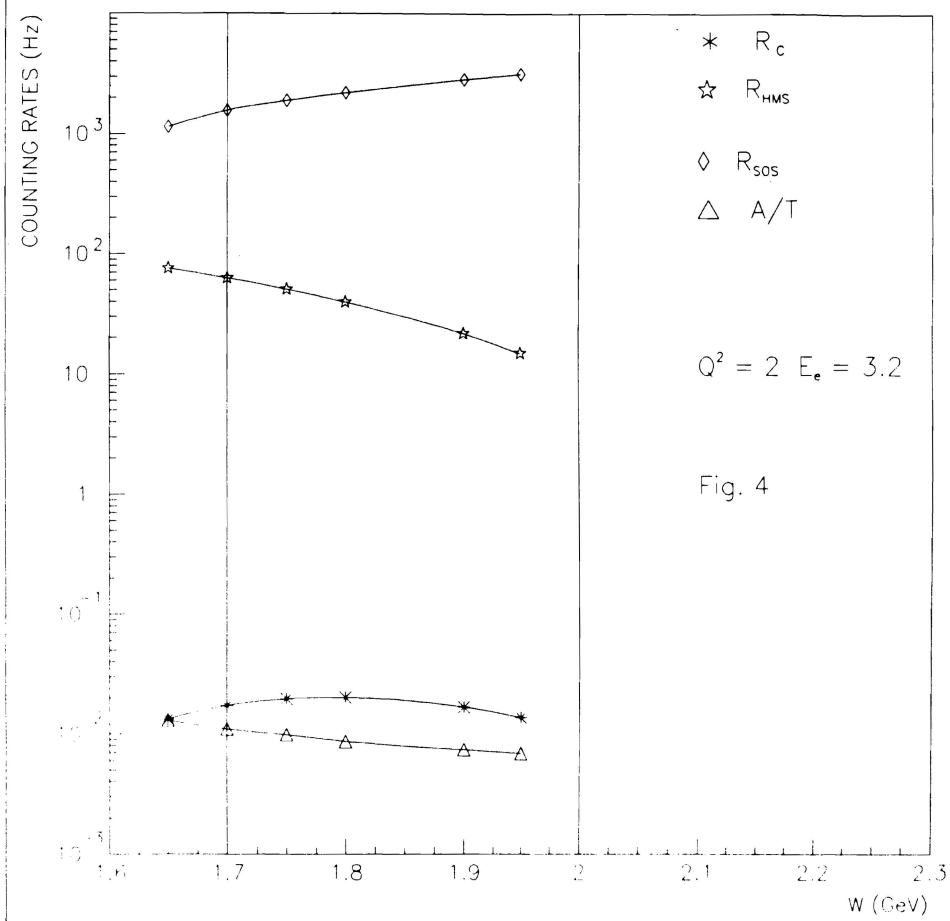
COUNTING RATES (Hz)
R_c
R_{HMS}
R_{SOS}
A/T
Q^2 = 2 E_e = 3.2
Fig. 4
W (GeV)